European Review for Medical and Pharmacological Sciences 2017; 21: 3705-3713

Effect of autophagy on myocardial infarction and its mechanism

Z. AISA[1], G.-C. LIAO[2], X.-L SHEN[1], J. CHEN[2], L. LI[1], S.-B. JIANG[1]

[1]Department of Cardiac Intensive Care Unit, Traditional Chinese Medicine Hospital of The Xinjiang Uygur Autonomous Region, Xinjiang, China
[2]Department of Intensive Care Unit, Traditional Chinese Medicine Hospital of The Xinjiang Uygur Autonomous Region, Xinjiang, China

Zulibiya Aisa and Guangchong Liao contributed equally

Abstract. – OBJECTIVE: To investigate the effect of autophagy on acute myocardial infarction (AMI), and its mechanism in rats.

MATERIALS AND METHODS: A total of 75 Sprague Dawley (SD) rats were randomly divided into three groups (n=25): sham operation (S) group, the AMI group and rapamycin (RAPA) treatment group. The model of AMI was established and the myocardial infarction size was calculated by triphenyltetrazolium chloride (TTC) staining. Morphological changes in myocardium were observed by hematoxylin and eosin (HE) staining. Expression levels of autophagy-related proteins LC3-phosphatidylethanolamine conjugate (LC3-II) and p62 were detected by semi-quantitative polymerase chain reaction (PCR) and Western blot.

RESULTS: Compared with the S group, the heart-to-body weight ratio on the 21st day in AMI group was significantly increased. TTC staining results showed that compared with the S group, the size of left ventricular infarction area was significantly increased in the AMI group, and that in the RAPA group was significantly decreased. HE staining results showed that the anterior wall of the left ventricle of rats became thinner, and myocardial cells were degenerated and lost seriously in the AMI group 21 days later. Compared with the S group, the expression level of LC3-II in the infarcted peripheral area was significantly increased and that of p62 was significantly increased in the AMI group. Compared with the AMI group, the expression level of LC3-II in the infarction-peripheral area was significantly increased and that of p62 was significantly decreased after the treatment with RAPA.

CONCLUSIONS: Autologous activation could protect myocardium by the left anterior descending (LAD) ligation in rats. Autophagy could reduce the area of myocardial infarction after LAD ligation and improve cardiac function.

Key Words:
Autophagy, AMI, Rapamycin, Rat.

Introduction

Coronary heart disease ranks first in current clinical causes of human death among other cardiovascular diseases, and acute myocardial infarction (AMI) is a severe acute type among coronary heart diseases[1,2]. The main etiological agents of AMI include the rupture, hemorrhage and thrombosis of coronary atherosclerotic plaques as well as the resulted severe luminal stenosis or occlusion caused by myocardial insufficiency or interruption. Besides, the size of the myocardial infarction area is closely related to the number of apoptotic myocardial cells and the prognosis of AMI patients[3-5]. At present, the most effective clinical treatment is to conduct revascularization for closed coronary arteries in the treatment window, clinically mainly including percutaneous coronary intervention and the bypass operation of coronary arteries, which, to a certain extent, reduce the occurrence and death rate of AMI[6-8]. Researchers have found that autophagy is involved in the pathogenesis of AMI as it can activate adenosine monophosphate-activated protein kinase (AMPK) by metformin to inhibit the activation of mammalian rapamycin target proteins. Autophagy can inhibit myocardial remodeling, improve cardiac function during AMI, and delay the development of AMI to heart failure[9]. Moreover, signal transducer and activator of transcription 1 (STAT1) deficiency increase autophagy in AMI so as to produce protective effect[10]. Howe-

Corresponding Author: Jiang Shubin, MD; e-mail: zuli510@163.com

ver, the action mechanism of autophagy in AMI is still not clear and needs further study. The primary purpose of this study was to investigate the role of autophagy in AMI and its mechanism by the AMI model of rats.

Materials and Methods

Instruments and Materials

TTC powders (Dingguo Changsheng Biotechnology Co., Ltd, Beijing, China); rabbit anti-p62, rabbit anti-LC3-II and rabbit anti-β catenin (Cell Signaling Technology, Inc., Danvers, MA, USA); electrogenerated chemiluminescence (ECL) liquid (Invitrogen, Carlsbad, CA, USA); developing powders (Invitrogen, Carlsbad, CA, USA); pipette (Eppendorf AG, Hamburg, Germany), electronic balances (BP121S, Sartorious AG, Gottingen, Germany), refrigerators (-80°C) (Thermo Fisher Scientific, Waltham, MA, USA), low temperature centrifuges (Thermo Fisher Scientific, Waltham, MA, USA), small animal ventilators (Techman Soft, Chengdu, China), epitheca of 18 G venous cannula needles of rat endotracheal intubation kit (Ningbo Medical Needle Co., Ltd., Ningbo, China); ophthalmic scissors, curved ophthalmic tweezers, straight tweezers, curved vascular clamps, gauze, medical cotton balls and sutures (Harbin Medical Apparatus Co., Ltd., Harbin, China); other involved instruments and reagents are described in relevant sections.

Experimental Animals and Grouping

A total of 75 male SD rats weighing 220±5 g were purchased from Xinjiang Medical University Laboratory Animal Center. This study was approved by the Animal Ethics Committee of Xinjiang Medical University Animal Center. Before the experiment, animals were adapted to the feeding environment for one week and followed the circadian rhythms, at the room temperature of 25°C; also, animals had meals and drunk water freely. 75 rats were randomly divided into three groups: the S group (n=25), the AMI group (n=25) and the RAPA group (n=25). On the second day after the model was established, we began to administrate drugs to these rats once a day and repeated this process for 21 days. On the 21st day, heart functions of these rats were detected by using high-resolution small animal ultrasound imaging system, and then they were executed and their hearts were taken out.

Establishment of AMI Model

Before the operation, we kept rats out from eating for 12 h, so their intestinal canals were empty and smooth. 10% chloral hydrate was injected into abdominal cavities of these rats to make them anesthetized. After they were in a stable narcosis, skins in the left chest were prepared, and the rats were fixed on the thermostat console. Cannulas were intubated into tracheas, and after the small animal ventilator was connected to assist breathing, we disinfected and cut skins in the area between the 3rd and 4th ribs in the left thorax. Next, we separated myometrium and made left ventricle and left atrial appendage exposed. The left anterior descending artery (LAD) was sutured at about 2 mm from the lower edge of the left atrial appendage, and the myocardium in the ligation area became white. Attenuated local myocardial motions, the overflowed left atrial appendage and accelerated and ST-segment elevation on the electrocardiogram (ECG), were regarded as signs of a successful ligation. After the ligation was indeed achieved, we closed thoracic cavities. After the operation, we conducted continuous intramuscular injection of penicillin (10,000 units per rat) (Yangtze River Pharmaceutical Group, Taizhou, China) for 3 days continuously. After heart rhythms and breathes of rats became steady, we stopped the assistance of mechanical ventilation and retained cannulas for observation. We pulled cannulas out after rats woke up and they were removed to the heating pad to observe rats for further 15 min. Then, these rats were fed in cages. 24 h after the operation, heat insulation treatment was conducted to rats. In the S group, we only conducted threading with no ligation for rats, but other operations were consistent with those in the AMI group.

Detection of Cardiac Functions

M-mode echocardiography was performed one day before the end of the experiment. Rats were put in the supine position under chloral hydrate anesthesia and fixed on a heating plate with the constant temperature 37°C. Their limbs and ECG electrodes were connected for the monitoring of heart rates and ECG records. Hair removal was conducted for left chest by chemical depilatory cream to reduce ultrasonic interference. The thoracic surface was coated with ultrasonic guidance agent for the optimization of the heart cavity environment and ultrasound detection. Left ventricular long-axis (LVALd) and left ventricular short-axis diameter at end diastole (LVIDs)

were measured, and left ventricular end-systolic and end-diastolic volumes (LVESV and LVEDV), left ventricular ejection fraction (LVEF) and left ventricular fractional shortening (LVFS) were calculated based on maximal and minimum cross-sectional areas and thicknesses.

Collection of Tissue Samples and Determination of Heart-to-Body Weight Ratio

On the 21st day, rats in all groups were weighed and intraperitoneally injected with 10% chloral hydrate. After the anesthesia, the hearts of them were removed and placed in cold phosphate-buffered saline (PBS). We kept the blood pump of cardiac chambers clean, washed away residual blood and dried the moisture with filter paper. We cut the heart with a sharp blade to isolate infarction-peripheral areas and placed the left parts in liquid nitrogen for 20 s; then, we put them in a refrigerator (-80°C) for preservation. Measurement method of the heart-to-body weight ratio of a rat: the heart weight was measured with a one-thousandth balance. The formula for calculating the heart-to-body weight ratio was as follows: heart weight ratio = rat heart weight/rat body weight ×100%.

Calculation of Myocardial Infarction Areas of Rats by TTC Staining

After the rats were anesthetized with 10% chloral hydrate, the inferior vena cava was cut, and the heart was rinsed from the aortic arch. Next, the heart was quickly removed. The residual blood was rinsed with cold PBS; the left ventricle was weighed and recorded; the left ventricle was cut into slices with the thickness of about 1-2 mm each, and each slice was weighted and recorded. Heart slices were placed in 1% triphenyltetrazolium chloride (TTC) phosphate buffer which was pre-heated to 37°C in a brown bottle (pH=7.4, the rinse was repeated for two times) and incubated in a dark incubator at 37°C for 15 min. The bottle was spun from time to time so that myocardial tissues evenly contacted with the staining solution. The infarction area became white and the non-infarction area became dark red after the staining. Stained myocardial slices were fixed in 4% paraformaldehyde for 30 min. After fixation, the images were taken and sizes of different stained areas were measured with image analysis software Image-ProPlus (Version X; Media Cybernetics, Silver Springs, MD, USA). The degree of myocardial infarction was expressed as the percentage between the weight of the infarction volume (white area) and the weight of the left ventricle.

Paraffin Sections of rat Cardiac Tissues

We took rat hearts into the cold heparin-containing PBS, washed away residual blood and fixed them with 4% paraformaldehyde for 18-24 h. After that, we removed tissues from the fixation solution and cut these hearts into two halves along the ligatures with a sharp blade and leave the ligatures in heart tips. Tissues received gradient alcohol dehydration according to the following order: 70% alcohol (1 h), 80% alcohol (1 h), 95% alcohol (2 times, 1 h/time) and 100% alcohol (3 times, 0.5 h/time). Then, these tissues were transparentized, waxed and embedded. After the dewaxing, they were washed with gradient alcohol to the hydration state. Tissues were stained by hematoxylin and washed by running water for 15-30 min. After tissues were stained by eosin, they received conventional dehydration and were transparentized and sealed.

Detection of the Expression Level of Relevant mRNA by Semi-Quantitative PCR

RNAs in cardiac tissues of rats in all groups were extracted by using TRIzol kits and their integrity was confirmed by agarose gel electrophoresis (AGE). The results showed that the 28S, 18S and 5S bands were clear and the brightness of the band 28S was about two times brighter than that of 18S, indicating that RNAs were intact and could be used for further experiments. Moreover, cDNAs were obtained from the reverse transcription by using reverse transcription kits, and expression levels of LC3-II and p62 were detected by semi-quantitative PCR with glyceraldehyde-3-phosphate dehydrogenase (GAPDH) as the internal reference. The reaction conditions were: 95°C for 30 s, 64°C for 25 s, 72°C for 30 s; there was a total of 35 cycles. Primers were synthesized by Tiangen Biotech Co., Ltd., (China). The sequence is shown in Table I, and after the reaction, the sequence was observed on the UV (ultraviolet) imaging system after receiving AGE.

Detection of Expression Levels of Relevant Proteins by Western blot

Radioimmunoprecipitation assay (RIPA) lysate was added in cardiac tissues extracted from rats at the ratio of 100 mg: 1 mL and the mixture was homogenized until there were no macroscopic tissues. After centrifugation at

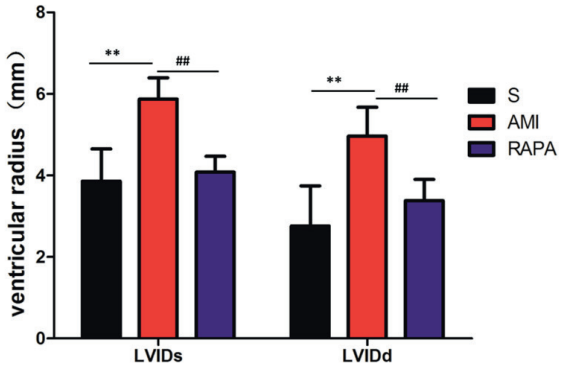

Figure 1. Changes in ventricular diameters in each group; LVIDs: left ventricular internal dimension in systole; LVIDd: left ventricular internal dimension at end diastole. Compared with the S group, LVIDs and LVIDd of rats are significantly increased in the AMI group ($^{**}p<0.01$). Compared with the AMI group, LVIDs and LVIDd of rats are significantly decreased in the RAPA group ($^{\#\#}p<0.01$).

12000 rpm for 10 min at 4°C, the supernatant was removed by DAB (3,3-diaminobenzidin) protein quantification kits (Invitrogen, Carlsbad, CA, USA). After that, sodium dodecyl sulfate polyacrylamide gel electrophoresis (SDS-PAGE) was performed and proteins were moved to the polyvinylidene difluoride (PVDF) membrane. After being blocked for 2 h, target bands were excised and incubated with LC3-II and p62 at 4°C overnight. The bands were washed with tris-buffered saline with tween-20 (TBST) for 3 times for 5 min each. Afterwards, second antibodies were incubated at room temperature for 2 h and washed with TBST for 3 times. Next, an appropriate amount of ECL liquid (a mixture of A liquid and B liquid in the ratio=1:1) was added in the dark room and tableting was performed. According to the fluorescence intensity of protein bands, the time of tableting was determined, and photographic fixing was conducted after the development. Finally, bands were scanned and their gray values were analyzed by ImageJ software.

Statistical Analysis

The data were analyzed by Statistical Product and Service Solutions (SPSS) 19.0 software (SPSS Inc., Chicago, IL, USA). The *t*-test was used to compare the data between the groups. The variance analysis was used to compare the data among several groups. After the variance homogeneity test, if the variance was homogeneous, the Bonferroni's method would be used for comparison, but if the variance was different, the Welch's method would be used for comparison. Multiple comparisons were analyzed by Dunnett's T3 method. $p<0.05$ was considered statistically significant.

Results

Changes in Cardiac Functions of Rats

Cardiac functions of rats in each group were measured on the 21st day after LAD ligation. Compared with the S group, LVIDs and LVIDd of rats were significantly increased in the AMI group ($p<0.05$ *vs.* Sham), and LVEF and LVFS of rats were significantly decreased ($p<0.01$). The autophagic activator rapamycin was intraperitoneally injected into rats on the 2nd day after LAD ligation. Compared with the AMI group, LVIDs and LVIDd of rats were significantly decreased ($p<0.01$), and LVEF and LVFS of rats were significantly increased in the RAPA group ($p<0.051$). The results are shown in Figure 1 and Figure 2 (A-B).

Changes in Heart-to-Body Weight Ratio of Rats

Heart-to-body weight ratios in each group were measured on the 21st day after LAD ligation. The results are shown in Figure 2C: compared with the S group, heart-to-body weight ratios of rats in the AMI group were significantly increased ($p<0.01$).

Table I. PCR primers.

	Sequences
LC3-II	Forward primer: 5'-ATCCAGAGACAAGACATGTAC-3' Reverse primer: 5'-TTCAGATGTTCTAAGCCTACGG-3'
p62	Forward primer: 5'-TGGCGGTTTGCGGTGGAC-3' Reverse primer: 5'-CCAGTGCAGGGTCCGAGGT-3'
GAPDH	Forward primer: 5'-GATGATTGGCATGGCTTT -3' Reverse primer: 5'-CACCTTCCGTTCCAGTTT-3'

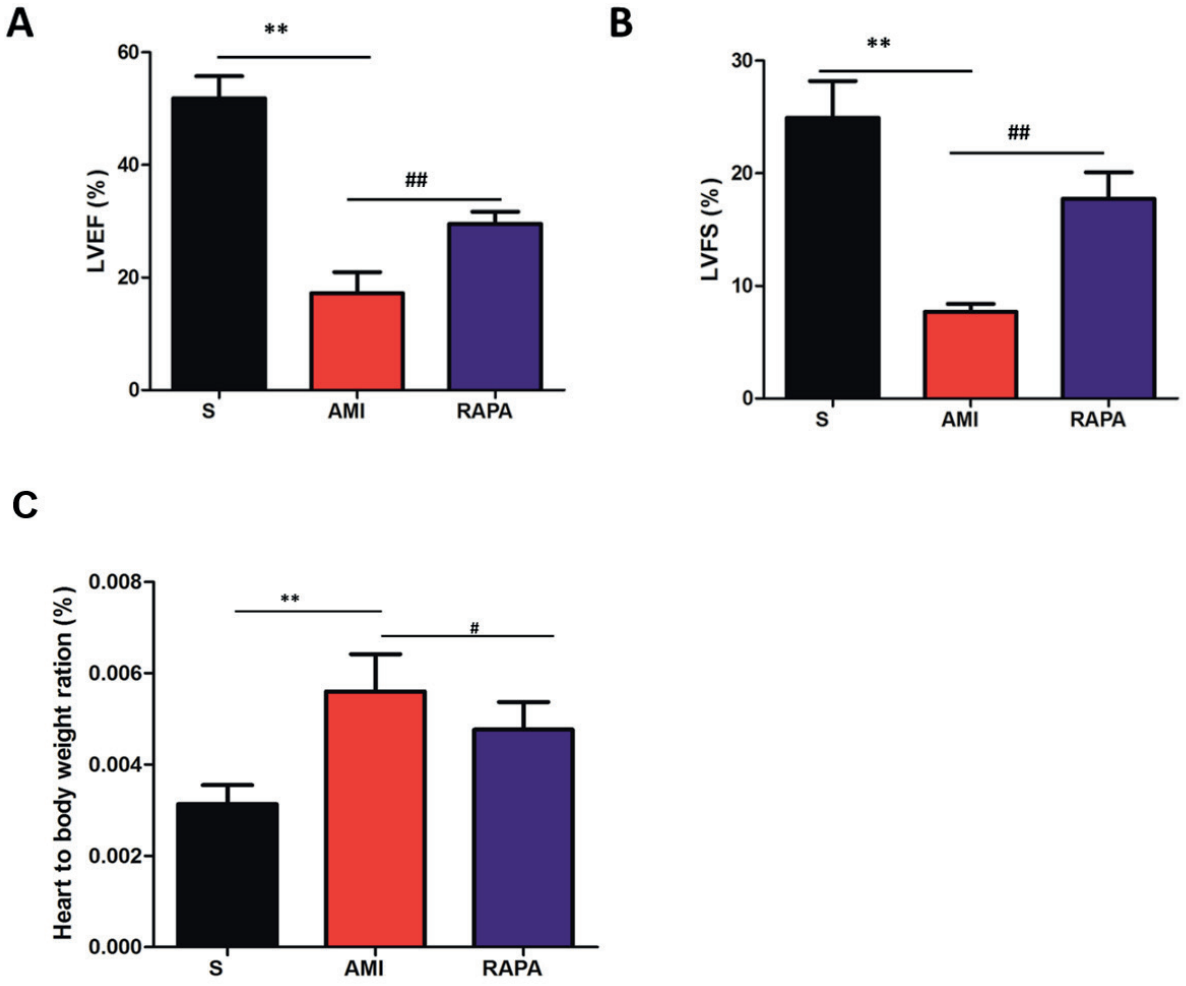

Figure 2. Changes in ventricular ejection fraction and the shortening of ventricular short axis in each group; LVEF: left ventricular ejection fraction; LVFS: left ventricular fractional shortening. ***A,*** shows changes in LVEF and ***B,*** shows changes in LVFS. Compared with the S group, LVEF and LVFS of rats are significantly decreased in the AMI group ($^{**}p<0.01$). Compared with the AMI group, LVEF and LVFS of rats are significantly increased in the RAPA group ($^{\#\#}p<0.01$). ***C,*** Changes in heart-to-body weight ratios of rats in each group. Compared with the S group, heart-to-body weight ratios of rats in the AMI group are significantly increased ($^{**}p<0.01$). Compared with the AMI group, heart-to-body weight ratios of rats in the RAPA group are significantly decreased ($^{\#}p<0.05$).

Compared with the AMI group, heart-to-body weight ratios of rats in the RAPA group were significantly decreased ($p<0.05$).

Changes in Myocardial Infarction Size of Rats

Hearts of rats were extracted on the 21st day after LAD ligation, and the infarction size of rats in each group was detected by TTC staining. The results are shown in Figure 3(A-B): compared with the S group, the size of rat left ventricular infarction was significantly increased in the AMI group ($p<0.01$). Compared with the AMI group, the size of rat left ventricular infarction was significantly decreased in the RAPA group ($p<0.01$).

Detection of Morphological Changes in the Infarction-Peripheral Area by HE Staining

HE staining was performed in the infarction-peripheral area to observe the changes in tissues in this area. The results are shown in Figure 3C: compared with the S group, the anterior wall of the left ventricle of rats became thinner, myocardial cells were degenerated and lost seriously, the remnant myocardial structure was destroyed and the fibroblasts were proliferated in the AMI group. Compared with the AMI group, the anterior wall of the left ventricle of rats became thickened, the arrangement of myocardial fibers was neat and the loss of myocardial cells was less in the RAPA group.

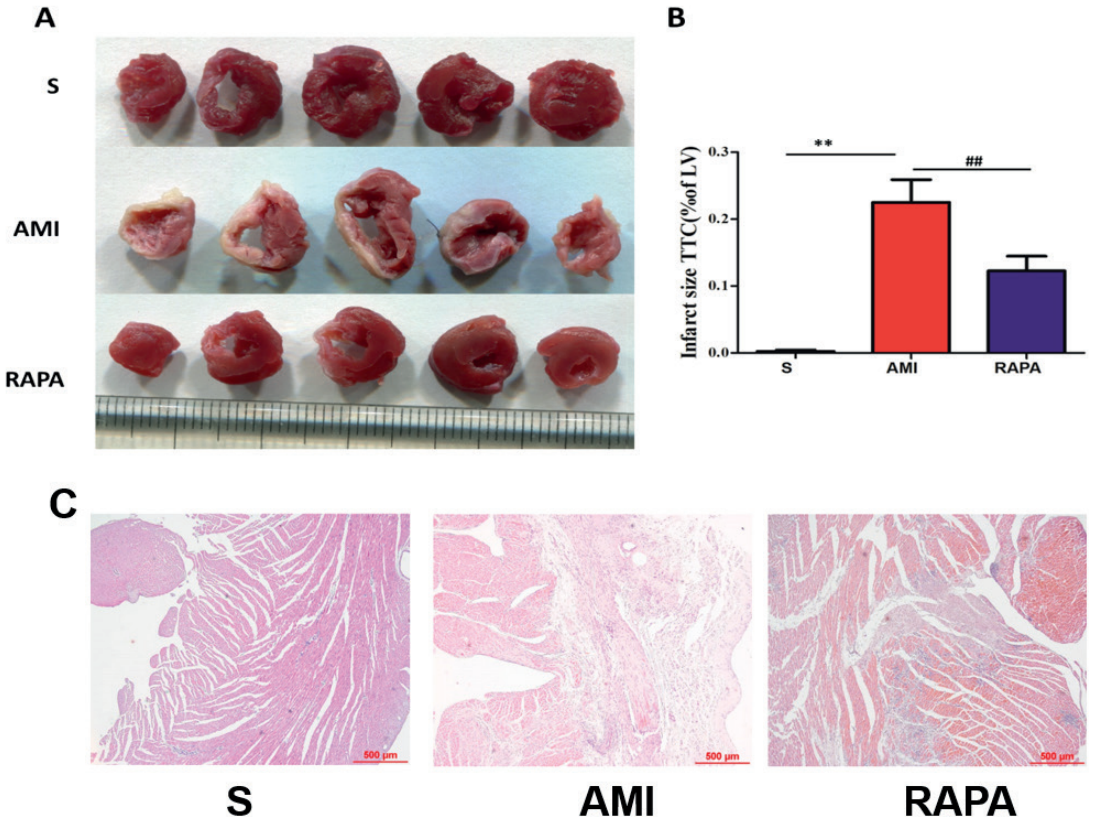

Figure 3. Comparisons of the myocardial infarction size of rats; ***A,*** is the picture of real TTC staining results and ***B,*** is the statistical graph of the infarction size. Compared with the S group, the size of rat left ventricular infarction is significantly increased in the AMI group ($^{**}p<0.01$). Compared with the AMI group, the size of rat left ventricular infarction is significantly decreased in the RAPA group ($^{\#\#}p<0.01$). ***C***, Morphological changes in the infarction-peripheral area after the operation in each group. Compared with the S group, the anterior wall of left ventricle of rats becomes thinner. Compared with the AMI group, the anterior wall of left ventricle of rats becomes thickened; bar=50 μm.

Detection of mRNA Expression Levels by Semi-Quantitative PCR

Expression levels of LC3-II and p62 mRNAs in the AMI group were detected by semi-quantitative PCR. The results are shown in Figure 4: compared with the S group, expression levels of LC3-II and p62 mRNAs in the AMI group were significantly increased and the differences were of statistical significance ($p<0.01$). Compared with the AMI group, expression levels of LC3-II and p62 mRNAs in the RAPA group were significantly decreased ($p<0.01$, $p<0.05$).

Detection of Expression Levels of Various Proteins by Western blot

Western blot was used to detect expression levels of LC3-II and p62 proteins. The results are shown in Figure 5: compared with the S group, expression levels of LC3-II and p62 proteins in the AMI group were significantly increased, and the differences were statistically significant ($p<0.01$). Compared with the AMI group, expression levels of LC3-II and p62 proteins in the RAPA group were decreased ($p<0.01$).

Discussion

The occurrence of AMI can lead to reduced blood perfusion and cause insufficient oxygen supply in the heart, thus resulting in the turning of a metabolic pathway of cardiomyocytes from aerobic metabolism to anaerobic glycolysis, reduced ATP synthesis, reduced energy supply, increased lactate, myocardial cell structure damage or death, weakened myocardial systolic and diastolic abilities, which will eventually lead to reduced systolic and diastolic function[11-14]. At present, most scholars believe that autophagy plays an important role in the occurrence and de-

velopment of cardiovascular disease. Crowell et al[15] discovered that AMPK is activated after cardiac ischemia by studying the role of autophagy in ischemia-reperfusion. The latter might inhibit mechanistic target of rapamycin (mTOR) activity so as to induce autophagy, thus playing a role in cardiomyocyte protection, but the reperfusion rapidly inactivated AMPK, thus damaging the heart[16]. A large number of recent studies have shown that autophagy plays the protective role in the ischemia of various organs. In this study, a rat AMI model was established by LAD permanent ligation. LAD ligation is able to mimic coronary artery occlusion with a short mold cycle. The greatest advantage is its good clinical relevance, which more fits for the clinical study of AMI pathological process. Therefore, it is the most commonly used preparation method for the AMI model. After the establishment of the AMI model, the success was assessed by echocardiographic testing, the heart-to-body weight ratio, myocardial infarction size and HE staining. The results showed that compared with the S group, LVIDs and LVIDd of rats were significantly increased in the AMI group, and LVEF and LVFS were significantly decreased. And heart-to-body weight ratios of rats in the AMI group were significantly higher than those in the S group. HE staining results also showed that the anterior wall of the left ventricle of rats became thinner, myocardial cells were degenerated and lost seriously, the remnant myocardial structure was destroyed and the fibroblasts were proliferated in the AMI group. The above results indicated that the rat AMI model was successfully established and AMI caused severe damages to the rat's heart shapes and functions. After the operation, rats were injected with RAPA for the assessment of cardiac functions in the AMI group. The results showed that compared with the AMI group, LVIDs and LVIDd of rats in the RAPA group were significantly decreased, but LVEF and LVFS of rats were significantly increased, indicating that cardiac functions of rats after receiving RAPA was recovered to a certain degree. In other words, activation of autophagy would improve cardiac functions of rats, showing that autophagy played a protective role in rat AMI.

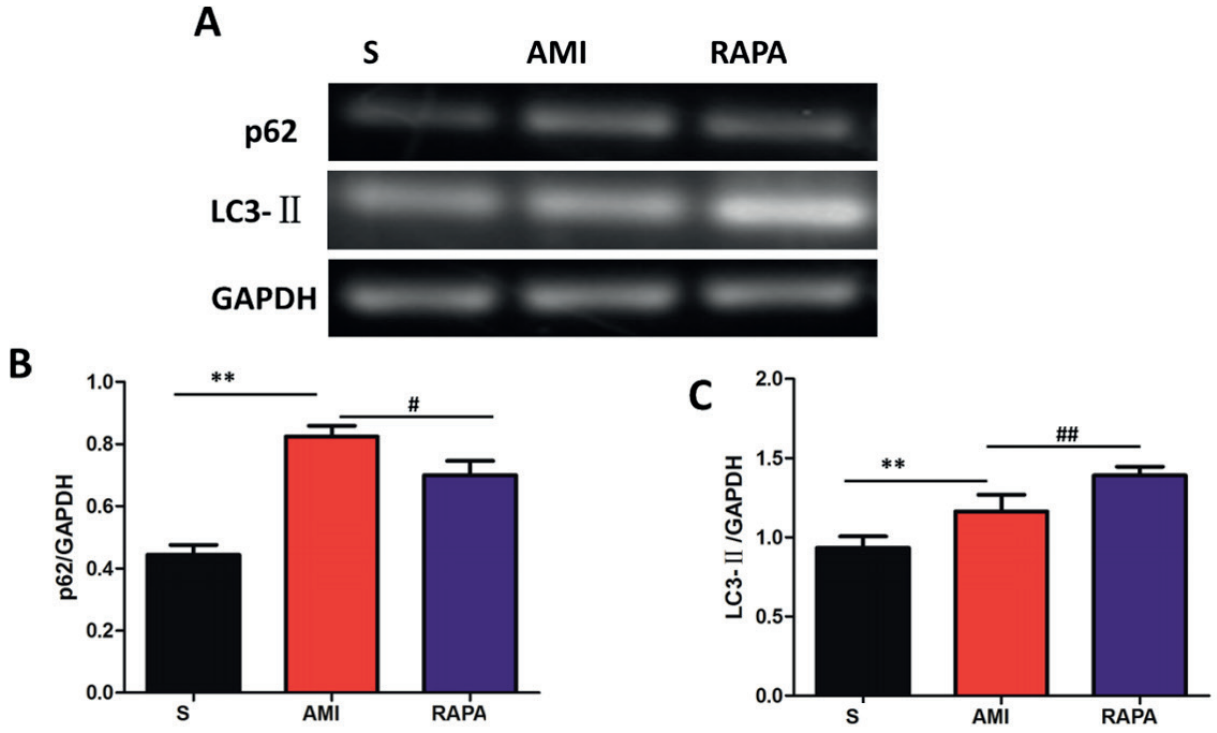

Figure 4. Detection of mRNA expression levels by semi-quantitative PCR. ***A*** is AGE, and ***B*** and ***C*** are statistical graphs of expression levels of p62 and LC3-II, respectively. Compared with the S group, expression levels of LC3-II and p62 mRNAs in the AMI group are significantly increased ($^{**}p<0.01$). Compared with the AMI group, expression levels of LC3-II and p62 mRNAs in the RAPA group are significantly decreased ($^{\#\#}p<0.01$, $^{\#}p<0.05$).

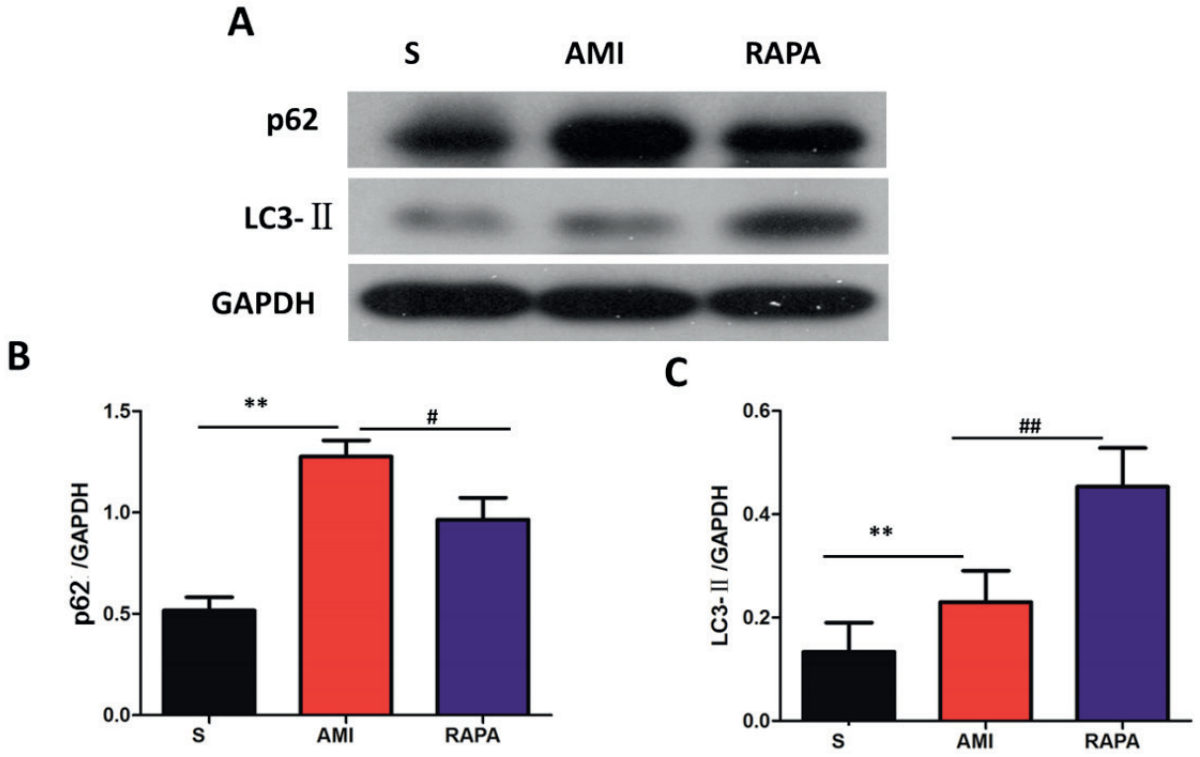

Figure 5. Detection of expression levels of LC3-II and p62 proteins by Western blot. ***A*** is the bar graph, and ***B*** and ***C*** are statistical graphs of expression levels of p62 and LC3-II, respectively. Compared with the S group, expression levels of LC3-II and p62 proteins in the AMI group are significantly increased ($^{**}p<0.01$). Compared with the AMI group, expression levels of LC3-II and p62 proteins in the RAPA group are decreased ($^{**}p<0.01$).

Expression levels of autophagy-related proteins were detected by semi-quantitative PCR and Western blot. The results showed that compared with the S group, the expression level of the autophagy-related protein LC3-II in the AMI group was significantly increased, and the expression level of autophagy substrate p62 was increased, indicating that AMI inhibited the autophagy in the body. The expression level of LC3-II was significantly increased and that of p62 was significantly decreased after the administration of autophagy activator RAPA, and the inhibition of autophagy in AMI was further confirmed by agonist. At the same time, it was found that cardiac functions of rats in the RAPA group were improved, indicating that enhanced autophagy protected the body in AMI I. Autophagy is a lysosome-involved catabolism process, mainly used for the recycling of macromolecules in the cell as well as the elimination of organelles and intracellular pathogens so as to maintain cell homeostasis, ensure that the cell energy supply and play the protective effect of cells[17-20].

Conclusions

In this study, it could be found from the rat AMI model that AMI could lead to changes in heart shapes and functions, and the damage of AMI to the heart could be reversed by activating autophagy, thus protecting the myocardial cells. This can provide a theoretical basis and a new direction for the clinical treatment of AMI.

Conflict of interest

The authors declare no conflicts of interest.

References

1) Khan JN, McCann GP. Cardiovascular magnetic resonance imaging assessment of outcomes in acute myocardial infarction. World J Cardiol 2017; 9: 109-133.

2) Sobieraj DM, White CM, Kluger J, Tongbram V, Colby J, Chen WT, Makanji SS, Lee S, Ashaye A, Coleman CI. Systematic review: Comparative effectiveness of adjunctive devices in patients with ST-segment

elevation myocardial infarction undergoing percutaneous coronary intervention of native vessels. BMC Cardiovasc Disord 2011; 11: 74.

3) Cho JS, Youn HJ, Her SH, Park MW, Kim CJ, Park GM, Jeong MH, Cho JY, Ahn Y, Kim KH, Park JC, Seung KB, Cho MC, Kim CJ, Kim YJ, Han KR, Kim HS. The prognostic value of the left ventricular ejection fraction is dependent upon the severity of mitral regurgitation in patients with acute myocardial infarction. J Korean Med Sci 2015; 30: 903-910.

4) Zhang WQ, Xie BQ. A meta-analysis of the relations between blood microRNA-208b detection and acute myocardial infarction. Eur Rev Med Pharmacol Sci 2017; 21: 848-854.

5) Kirchberger I, Wolf K, Heier M, Kuch B, von Scheidt W, Peters A, Meisinger C. Are daylight saving time transitions associated with changes in myocardial infarction incidence? Results from the German MONICA/KORA Myocardial Infarction Registry. BMC Public Health 2015; 15: 778.

6) Colombo MG, Meisinger C, Amann U, Heier M, von Scheidt W, Kuch B, Peters A, Kirchberger I. Association of obesity and long-term mortality in patients with acute myocardial infarction with and without diabetes mellitus: Results from the MONICA/KORA myocardial infarction registry. Cardiovasc Diabetol 2015; 14: 24.

7) Chen H, Xu Y, Wang J, Zhao W, Ruan H. Baicalin ameliorates isoproterenol-induced acute myocardial infarction through iNOS, inflammation and oxidative stress in rat. Int J Clin Exp Pathol 2015; 8: 10139-10147.

8) Chapman AR, Adamson PD, Mills NL. Assessment and classification of patients with myocardial injury and infarction in clinical practice. Heart 2017; 103: 10-18.

9) Wu X, He L, Chen F, He X, Cai Y, Zhang G, Yi Q, He M, Luo J. Impaired autophagy contributes to adverse cardiac remodeling in acute myocardial infarction. PLoS One 2014; 9: e112891.

10) Zhang Z, Yang C, Shen M, Yang M, Jin Z, Ding L, Jiang W, Yang J, Chen H, Cao F, Hu T. Autophagy mediates the beneficial effect of hypoxic preconditioning on bone marrow mesenchymal stem cells for the therapy of myocardial infarction. Stem Cell Res Ther 2017; 8: 89.

11) Hajsadeghi S, Chitsazan M, Chitsazan M, Haghjoo M, Babaali N, Norouzzadeh Z, Mohsenian M. Metabolic syndrome is associated with higher wall motion score and larger infarct size after acute myocardial infarction. Res Cardiovasc Med 2015; 4: e25018.

12) Huang R, Yao K, Sun A, Qian J, Ge L, Zhang Y, Niu Y, Wang K, Zou Y, Ge J. Timing for intracoronary administration of bone marrow mononuclear cells after acute ST-elevation myocardial infarction: A pilot study. Stem Cell Res Ther 2015; 6: 112.

13) Al-Salam S, Hashmi S. Galectin-1 in early acute myocardial infarction. PLoS One 2014; 9: e86994.

14) Liebetrau C, Weber M, Tzikas S, Palapies L, Mollmann H, Pioro G, Zeller T, Beiras-Fernandez A, Bickel C, Zeiher AM, Lackner KJ, Baldus S, Nef HM, Blankenberg S, Hamm CW, Munzel T, Keller T. Identification of acute myocardial infarction in patients with atrial fibrillation and chest pain with a contemporary sensitive troponin I assay. BMC Med 2015; 13: 169.

15) Liu J, Wu P, Wang Y, Du Y, A N, Liu S, Zhang Y, Zhou N, Xu Z, Yang Z. Ad-HGF improves the cardiac remodeling of rat following myocardial infarction by upregulating autophagy and necroptosis and inhibiting apoptosis. Am J Transl Res 2016; 8: 4605-4627.

16) McCormick J, Suleman N, Scarabelli TM, Knight RA, Latchman DS, Stephanou A. STAT1 deficiency in the heart protects against myocardial infarction by enhancing autophagy. J Cell Mol Med 2012; 16: 386-393.

17) Yan W, Guo LR, Zhang Q, Sun WZ, O'Rourke ST, Liu KX, Sun CW. Chronic blockade of class I PI3-kinase attenuates Ang II-induced cardiac hypertrophy and autophagic alteration. Eur Rev Med Pharmacol Sci 2015; 19: 772-783.

18) Netea-Maier RT, Plantinga TS, van de Veerdonk FL, Smit JW, Netea MG. Modulation of inflammation by autophagy: consequences for human disease. Autophagy 2016; 12: 245-260.

19) Kubli DA, Gustafsson AB. Cardiomyocyte health: adapting to metabolic changes through autophagy. Trends Endocrinol Metab 2014; 25: 156-164.

20) Li Z, Wang J, Yang X. Functions of autophagy in pathological cardiac hypertrophy. Int J Biol Sci 2015; 11: 672-678.